Distribution and Turnover Rate of Acetylcholine Receptors throughout the Junction Folds at a Vertebrate Neuromuscular Junction

MIRIAM M. SALPETER and ROSE HARRIS
Section of Neurobiology and Behavior, Cornell University, Ithaca, New York 14853

ABSTRACT The distribution and turnover rate of acetylcholine receptors labeled with ^{125}I-α-bungarotoxin were examined in innervated mouse sternomastoid muscle by electron microscope autoradiography using the "mask" analysis procedure. We compared the total population of receptors with receptors newly inserted at the junction 2 d after inactivation with nonradioactive α-bungarotoxin, both at the top (thickened) region of the postjunctional folds (pjm) and the nonthickened bottom folds. We found that the receptor site density was ~10 times greater on the thickened pjm than on the nonthickened bottom folds for both total and newly inserted receptors. This ratio does not change significantly during a 6-d period after labeling the new receptors. Furthermore, calculated values for turnover time of receptors show that both total and newly inserted receptors at both regions of the junctional folds have half-lives for degradation within the range given in the literature for slow junctional receptors. These data exclude a simple migration model whereby receptors are preferentially inserted in the nonthickened region of the junctional folds and then migrate into the thickened membrane at a rate equal to the turnover rate of the receptors.

The postsynaptic folds of the vertebrate neuromuscular junction are heterogeneous in terms of both receptor distribution and morphology. The top ~2,000 Å of postjunctional membrane (pjm) has a distinct electron density, a cytoplasmic filamentous substructure (4) and is rich in intramembrane particles (13, 26, 28). This thickened region has a high density of receptors (~10,000–20,000 sites/μm^2) (2, 15, 16, 19, 23, 27). At the bottom of the folds, the membrane is morphologically indistinguishable from that at extrajunctional regions, and the receptor site density is considerably reduced (~1,000 sites/μm^2, or ~5–10% the site density at the top of the folds). This site density is equivalent to that seen in the perijunctional region, 0.5–1 μm immediately surrounding each axonal end bouton (16).

The reason for the heterogeneity in the organization of the pjm has not yet been established. Much is known about the properties of extrajunctional and junctional receptors both during development and after denervation (for review see references 10, 14). However, nothing is known about the properties of the acetylcholine receptor (AChR) at the bottom, nonthickened region of the pjm. In the present study, we asked two questions: (*a*) Do the AChRs in the nonthickened bottom folds resemble extrajunctional or embryonic receptors in having a fast turnover rate, and (*b*) do the nonthickened bottom folds provide a region for the insertion of AChRs that subsequently migrate to the thickened pjm?

We used innervated mouse sternomastoid muscle to examine both the localization and turnover rate of junctional receptors at the top thickened pjm and at the bottom nonthickened membrane. We did this for the total population of receptors as well as for receptors newly inserted at the junction during a 2-d period. We found that the turnover rate of total and newly inserted AChRs in both the top and bottom of the pjm are within the range given by others for innervated junctional AChR. We further found that there is no apparent preferential localization of newly inserted receptors in the bottom vs. the top of the folds. This suggests that during turnover of adult junctional receptors there is a rapid equilibration of receptor location to maintain a steady state throughout the entire membrane.

MATERIALS AND METHODS

We used female mice (Albino, Blue Spruce Farms Inc., Altamont, NY). The sternomastoid muscle was exposed under Nembutal anaesthesia and the receptors were saturated with α-bungarotoxin (BTX) as previously described (16, 22). The α-bungarotoxin was purified and iodinated as in Loring et al. (21). Three experimental protocols were: (*a*) The muscle was bathed with ^{125}I-BTX for 3 h to saturate all receptors, briefly washed in Krebs Ringer's, and then fixed in situ when the animal was perfused intracardially with 4% paraformaldehyde in phosphate buffer. This group was called "total, zero time." (*b*) The muscle was bathed for 3 h in nonradioactive toxin to saturate all receptors. 2 d later, the muscle was exposed again and bathed with ^{126}I-BTX for the same length of time in order to saturate all new receptors that had been inserted during the 2-d

period. The animals were fixed immediately after labeling. This group was called "new, zero time." (*c*) The third group of animals was treated as were those in group 2, but after saturating the new receptors with ^{125}I-BTX the animals were allowed to survive for 1, 4, or 6 d, in order to determine the fate of the newly inserted receptors.

Preparing Tissue: After fixation, the muscle regions containing the endplates were cut up, postfixed in 1% OsO_4 for 1 h, block-stained in 2% uranyl acetate (1 h at room temperature), dehydrated in graded ethanol, and embedded in Epon 812. The tissue was then sectioned and prepared for electron microscopic (EM) autoradiography by the flat substrate procedure of Salpeter and Bachmann (32–34), using Ilford L4 emulsions and D19 development.

Analysis of Autoradiograms: We used only autoradiograms of endplate regions in which all the membranes were seen as distinct lines, indicating that the membranes were cut at right angles to the plane of the membrane (Fig. 1). The EM autoradiograms were analyzed by using the mask analysis as previously described (35, 36). We first separated the postjunctional folds into two postulated sources (called source compartments): (*a*) the thickened region of the postjunctional membrane at the top ~2,000 Å of the folds (identified morphologically) and (*b*) the nonthickened bottom folds. This allowed us to compare site density and turnover times for receptor in these two distinct regions of the pjm and to determine whether new receptors are preferentially located in either one of these regions. An interface source was also analyzed separately as described in the text.

To use the mask analysis with linear sources, we had to modify the procedure slightly over that previously used (35, 36). We first generated random, assumed point sources with a known average spacing along the membranes. This was done by placing a grid over the endplate and registering a source at every intersection between a grid line and the membrane source compartment. (The average distance between sources is then given by $\pi/4 \times d$, where d is the spacing of the grid.)

To generate an expected source to grain matrix, the sources of each mask source-to-grain pair were laid over these assumed membrane point sources (while keeping the masks at a constant orientation). For each source, the location of the generated grain was marked. (This was done using a computer but can also be done by hand.) A different source-to-grain pair was used for each consecutive, assumed point source on the membrane until all source-to-grain pairs were used, and the sequence was begun again. This procedure is similar to that used for validating the mask analysis on an assumed line source in Salpeter et al. (36). (A detailed description of the use of masks for line sources is in press: Salpeter, M. M., et al. 1983. *J. Electron Microsc. Techn.*)

For each generated grain and each observed developed grain, the shortest distance to the axonal membrane was measured. Based on these measurements, the generated and observed grains were then tabulated in specific grain compartments consisting of six bands of unequal widths, parallel to the axonal membrane, as follows (negative values are into axon; positive values towards muscle): compartment 1 went from −1,000 Å to +950 Å; 2, from 950 Å to 1,580 Å; 3, from 1,580 Å to 2,420 Å; 4, from 2,420 Å to 4,030 Å; 5, from 4,030 Å to 5,540 Å and 6, from 5,540 Å to 10,500 Å.

An χ^2 minimization program (as reported in previous publications; see appendix to reference 36) was used to derive a set of relative site densities for the postulated source compartments, such that the expected grains generated from these source compartments give the best fit to the experimentally observed distribution of developed grains in the autoradiograms. These relative optimized source densities are, in effect, grain densities that have been corrected for radiation spread. We then used these corrected grain densities to calculate the AChR sites/μm^2 of membrane using the equation given previously (16, 23), taking into consideration the specific activity of the bungarotoxin, the exposure time, the tested sensitivity of the emulsion, the thickness of the section, and the spacing of the assumed point sources along the membrane.

RESULTS

Fig. 1 illustrates an EM autoradiogram such as was used for the analysis. Tables I and II and Fig. 2 give the receptor site densities at the thickened pjm and the bottom folds for total receptors and for receptors newly inserted during a 2-d period. Data are also given for the degradation of these newly inserted receptors during a period of 6 d.

Turnover of Receptors

Our data allowed us to get estimates of turnover time for the AChR at the top thickened pjm and at the nonthickened bottom of the folds for both the total and newly inserted receptors. To obtain the half-life of total receptors ($t_{1/2tot}$), we compared the number of receptors immediately after labeling all receptors with ^{125}I-BTX, (R_o) (total receptors; zero time), with the number labeled 2 d after inactivation with nonradioactive toxin, (R_n) (new receptors; zero time), using the equation

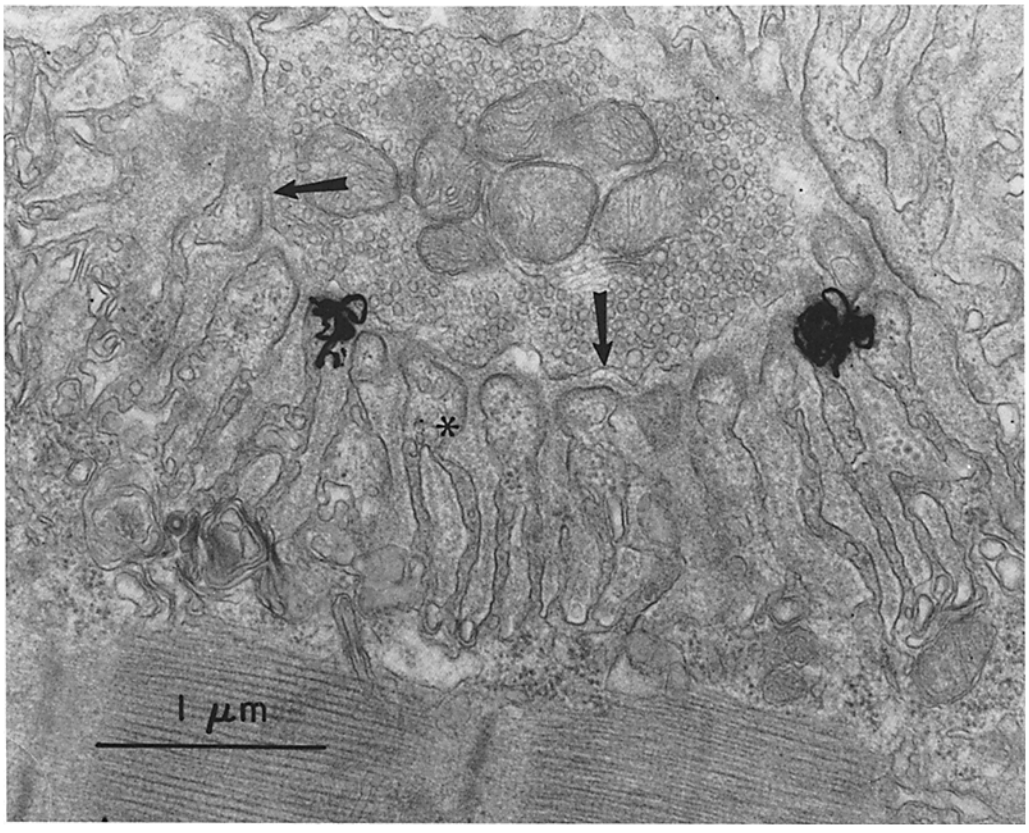

FIGURE 1 EM autoradiogram of endplate of mouse sternomastoid muscle, illustrating the requirements for inclusion in the analysis. The region between the arrows shows tissue with crisp membranes such as were tabulated in this study. The rest illustrates regions with tangential membranes that would be excluded from the analysis. The asterisk marks the bottom of the thickened pjm on one fold. The "interface source compartment" included 1,000 Å above and below this mark.

$t_{1/2} = (\ln 2)\,(t)\,[-\ln (R_r/R_o)]^{-1}$, where R_r, the value for residual receptors, was $R_o - R_n$ (R_n being derived from the y-intercept in Fig. 2), and t is the decay time (which was 2 d in this study). The $t_{1/2tot}$ obtained for the receptors on the thickened pjm was 8.5 d and that on the nonthickened bottom folds was 6.7 d.

The half-life for the new receptors that had been inserted during a 2-d period, $t_{1/2new}$, was obtained by linear regression from the semilogarithmic plot (Fig. 2) of data from nine animals, assuming a single exponential. The values were 6.8 and 5.2 d for the thickened top pjm and the nonthickened bottom folds, respectively. Thus, the $t_{1/2}$ values obtained for total and newly inserted receptor, both at the top and bottom of the junctional folds, are all within the range of values previously reported for innervated junctional receptors (3, 6, 7, 9, 18, 20, 22, 24, 25, 30, 31, 39, 41) and can thus all be classified as representing "slow" turnover relative to the values of 10–30 h usually reported for the embryonic or postdenervation receptors undergoing "fast" turnover (1, 3, 9, 11, 12, 24, 31, 37, 38, 41). The range in the $t_{1/2}$ values from ~8.5 d for the total receptors at the thickened pjm to the ~5.2 d for the newly inserted receptors at the bottom folds needs comment and will be dealt with in the Discussion.

Possible Sites of Insertion of New Receptors

Weinberg et al. (42) have reported that at developing ectopic endplates, receptors are inserted in a rim at the periphery of the junction, and that these receptors then move towards the center of the junction. We will call this the migration model. Our data allowed us to ask whether such a migration of newly inserted receptors occurs also at the adult innervation junction. We have previously seen that newly inserted receptors appear throughout the neuromuscular junction (17, 22). Therefore, it seemed very unlikely that there would be a rim at the periphery of the entire neuromuscular junction that would provide an insertion zone for new receptors in the adult junction. However, our earlier studies did not do a thorough analysis to test whether there may be local insertion rims. We therefore asked whether the nonthickened bottom folds may provide such an insertion zone.

If the receptors are inserted at the nonthickened bottom folds and move up, then this movement should be reflected in the ratios of the receptor site densities in the thickened pjm to that at the nonthickened bottom folds at different times after labeling the newly inserted receptors. Tables I and II show that the ratio of BTX binding site density in the thickened pjm to that at the bottom is 10 to 1 and is about the same for total receptors and newly inserted receptors. Furthermore, this ratio stays essentially constant over the 6-d period after labeling the new receptors.

Because of the steady state maintained in overall receptor

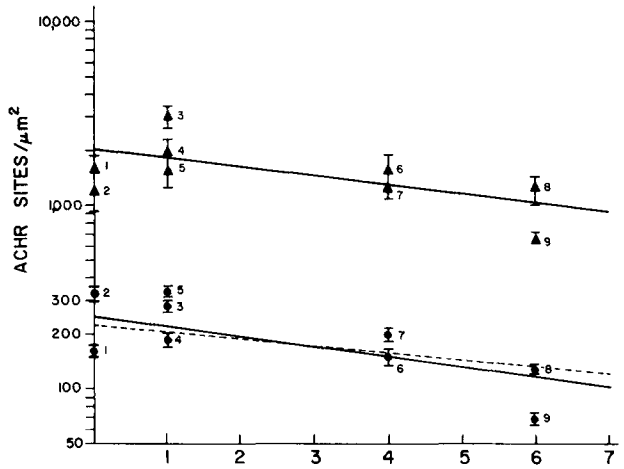

FIGURE 2 Semi-logarithmic plot giving degradation time course of new receptors. Receptors had been saturated with nonradioactive BTX, and 2 d later all newly inserted receptors were saturated with ^{125}I-BTX. Animals were fixed either immediately (zero time in present figure) or up to 6 d later and site densities were determined by EM autoradiography. Plots of the individual AChR site densities are shown at the thickened pjm (▲) at the top of the junctional folds or at the nonthickened bottom folds (●). Nine animals were used for this sequence and the individual values obtained from each animal were numbered to allow a comparison between the value at the top and that at the bottom of the folds. The best fit lines (solid lines) were obtained by linear regression and give $t_{1/2}$ values of 6.7 d at the thickened pjm and 5.2 d at the bottom folds, respectively. The error range represents an SEM for each value and comes from the χ^2 minimization routine used with the mask analysis (36). Broken line is for a half-life of 8 d for comparison. Both functions are monoexponential.

TABLE I

Total Receptors: Distribution and Turnover

Location/time	(AChR sites/μm²) × 10⁻³ Zero time*	2 d‡	$t_{1/2tot}$§
Thick pjm	13.0 ± 1.3	11.1 ± 2.4	8.5
Nonthick bottom fold	1.2 ± 0.3	0.98 ± 0.3	6.7
Ratio‖ of site densities	10.7 ± 2.9	11.0 ± 4	—

* Total receptors at zero time are all receptors at junction seen after labeling with ^{125}I-BTX. Data are pooled from two animals and more than 100 grains per animal. Site density was calculated as described in text. Error ranges are derived from χ^2 minimization (36).

‡ Residual receptors 2 d after labeling were derived by subtracting new receptors 2 d after cold BTX (y-intercept Fig. 2) from total receptors immediately after labeling with hot BTX (zero time). Error ranges are relatively larger than for zero time since they are the combined error from the y-intercept and the zero-time value.

§ The $t_{1/2tot}$ is half-life for total receptors derived as described in text.

‖ Ratio is of site densities at thickened pjm to that at bottom fold.

TABLE II

New Receptors: Distribution and Turnover*

Location/time	(AChR sites/μm² × 10⁻³) 0	1 d	4 d	6 d	$t_{1/2new}$‡
Thick pjm	1.47 ± 0.18	2.34 ± 0.23	1.41 ± 0.12	0.89 ± 0.08	6.8
Nonthick bottom fold	0.18 ± 0.04	0.26 ± 0.07	0.14 ± 0.04	0.09 ± 0.02	5.2
Ratio§	8.4 ± 2.3	9 ± 2.5	10.1 ± 3.2	10.1 ± 2.8	—

* New receptors are receptors inserted during a 2-d period after saturating all receptors with nonradioactive BTX ± SEM. Each data point is value pooled from 2 to 3 animals (see Fig. 2) and more than 100 grains per animal.

‡ $t_{1/2new}$ is half-life of new receptors derived by linear regression from Fig. 2.

§ Ratio is of site density at thickened pjm to that at nonthickened bottom folds.

number, the net migration of receptor has to have the same half-life as receptor turnover, which for our data would be ~7 d. A more sensitive test of the migration model would then be to identify a separate interface source compartment that would include the assumed insertion region and an amount of thickened pjm that would be greater than the length over which receptors would move in 2 d. With a half-life of ~7 d, this will be ~17% of the distance up the thickened pjm and even less than that distance if the true half-life were 10 d. In either case, at least the top 80% of the thickened pjm should be unlabeled at new zero time. To test this migration hypothesis further, we subdivided the thickened pjm into two regions, each being included in a different postulated source compartment. The bottom 1,000 Å of thickened pjm (which constitutes ~30% of total thickened membrane) was combined with 1,000 Å of the nonthickened membrane (just below the thickened membrane) (see Fig. 1). This interface region was designated as source compartment 1. The top 1,000 Å of thickened pjm that includes the region parallel to the axon and thus ~70% of the thickened pjm was designated as source compartment 2. If the migration model is right, source 1 should contain all the label and source 2 should be unlabeled at "new zero time." We found, however, that at "new zero time" the site densities in sources 1 and 2 were 1,251 ± 233 and 975 ± 247 AChR sites/μm^2 of membrane, respectively. The fact that there is a significant label (>3 SEM above zero) in source compartment 2, 2 d after saturating all receptors with cold BTX, argues against the simple migration model.

DISCUSSION

Insertion of New Receptors

New receptors do not appear to be preferentially inserted at the bottom of the folds with a subsequent net migration upward into the thickened pjm at a rate equal to the degradation rate. This can be seen from the ratio of sites per square micrometer at the thickened and nonthickened membranes (Tables I and II) and from the result given in the text that there is a high positive label at the top of the thickened pjm (source compartment 2) at new zero time. (A similar conclusion was reached in an earlier study [17].) In that sense, the adult innervated junction appears to differ from the developing ectopic junction (42).

The question of how the AChR degradation and insertion occurs remains unanswered. It has previously become obvious that the high, steady-state number of junctional receptors, especially after denervation when turnover is very fast (5, 20, 22), requires a mechanism of selective insertion of receptors at or near the endplate. Some investigators have implicated vesicles in the insertion of AChR (8, 29). The morphology of the adult junction (e.g., Fig. 1) shows that most vesicles are in the region of the nonthickened bottom folds and at the interface with the thickened pjm, but not at the top of the folds where the receptors are most numerous. However, on the average over the entire pjm, an 8-d half-life means that per hour <20 receptors are inserted per square micrometer of pjm surface area (or per 10 μm membrane length on the micrograph). Thus, most of the vesicles seen on the micrographs are probably not involved in receptor turnover. We thus cannot argue either in favor or against vesicular insertion of receptors nor on the exact location of such insertion. Even though we reject a simple migration model, it is still possible that receptors are inserted, possibly via vesicles, at the interface or anywhere in the membrane, and that these newly inserted receptors are at first freely mobile and quickly redistribute throughout the junction. The 10 to 1 ratio of receptor localization at the top and bottom of the junctional folds could then reflect a ratio of receptor anchoring sites. Such a model is not experimentally distinguishable from one that postulates a one for one replacement of receptors throughout the junctional folds. Thus the mechanism of receptor insertion coupled to degradation, in order to maintain the steady state of receptors, still needs to be determined.

Turnover Rate of Innervated Junctional Receptors

TOTAL RECEPTORS: In this study of the adult innervated junction, the total receptors both at the thickened pjm and at the bottom folds turn over with a half-life of >5 d and are within the range of values given for slow junctional receptors (3, 6, 7, 9, 18, 20, 22, 30, 31, 41). Since the turnover of receptors at the bottom folds is slow, this population cannot be equated with postdenervation extrajunctional type receptors, even though their site density is low. Thus, in the innervated sternomastoid muscle, the AChRs that are present, independent of localization or site density, appear to have a slow turnover rate. We do not yet know the mechanism(s) whereby the nerve controls receptor turnover rate at the innervated junction while maintaining the steady state in site density. Whatever the mechanisms may be, our results show that neither a morphologically obvious membrane specialization nor very high receptor concentrations (i.e., >10,000 sites/μm^2) are necessary correlates of slow turnover.

NEW RECEPTORS: One conclusion from our data is that during turnover of receptors at innervated junctions, the bulk of the newly inserted receptors have a long half-life within the range of values reported for the total populations at this junction. Our actual measured half-lives at the bottom of the folds are shorter than those at the tops of the folds, and in each region half-lives of the new receptors are slightly shorter than those of the total receptors (i.e., at the thickened pjm the $t_{1/2}$ for total receptors is 8.5 d and that of new receptors is 6.8 d, while at the bottom folds the $t_{1/2}$ values were 6.7 and 5.2 d for total and newly inserted receptors, respectively). Given the animal-to-animal variation, none of these values is significantly different from an 8-d half-life (as the dashed curve on Fig. 2 illustrates), and all receptors' half-lives may be equally long. Stanley and Drachman (40) have recently suggested that newly inserted receptors at the neuromuscular junction have a short half life, using as evidence the fact that receptors labeled 6 d after inactivation with cold BTX have an average half-life of ~3.5 d. According to this assertion, our new receptors, being only 2-d old, should have an even faster average half-life than 3.5 d, which is incompatible with our data. However, it is possible that the slightly shorter half-life at the bottom of the folds for newly inserted receptors may reflect the presence of a small population of binding sites with a short half-life. These could be either uniformly distributed nonspecific sites or newly inserted, specific receptor sites as suggested by Stanley and Drachman (40). If a small number of such sites exist, their influence on the apparent half-life would be greater wherever the overall receptor number is lower, i.e., at the bottom of the folds, and for newly inserted receptors. For instance, 50 fast sites per square micrometer would shift an observed half-life for newly inserted receptors at the bottom of the folds from 8 to 5.4 d. The question of whether our $t_{1/2}$ values reflect statistical variation or the presence of a fraction of fast receptors remains unanswered. The monoexponentials in Fig. 2 and the

argument given above indicate that if there are any rapidly decaying BTX binding sites their number must be <50 sites per square micrometer.

In conclusion, in the adult innervated junction there appears to be no obvious net movement of receptor either up or down the junctional folds during turnover. A steady state of receptor density is maintained throughout the junctional folds as is an overall slow turnover rate.

We wish to thank Jeffrey Goldner for the computer programming, William Harris for preparing illustrations, and Patricia Scattergood for help with photography and for typing the manuscript.

This work is supported by NIH grant NS 09315.

Received for publication 17 December 1982, and in revised form 4 March 1983.

REFERENCES

1. Appel, S. H., R. Anwyl, M. W. McAdams, and S. Elias. 1977. Accelerated degradation of acetylcholine receptor from cultured rat myotube with myasthenia gravis sera and globins. *Proc. Natl. Acad. Sci. USA.* 74:2130–2134.
2. Bader, D. 1981. Density and distribution of α-bungarotoxin binding sites in postsynaptic structures of regenerated rat skeletal muscle. *J. Cell Biol.* 88:338–345.
3. Berg, D. K., and Z. W. Hall. 1975. Loss of α-bungarotoxin from junctional and extrajunctional acetylcholine receptors in rat diaphragm muscle *in vivo* and in organ culture. *J. Physiol. (Lond.)* 252:771–789.
4. Birks, R. I. 1966. The fine structure of motor nerve endings at frog myoneural junctions. *Ann. NY Acad. Sci.* 135:8–26.
5. Brett, R. S., S. G. Younkin, M. Konieczkowski, and R. M. Slugg. 1982. Accelerated degradation of junctional acetylcholine receptor-α-bungarotoxin complexes in denervated rat diaphragm. *Brain Res.* 233:133–142.
6. Burden, S. 1977. Development of the neuromuscular junction in chick embryo: the number, distribution, and stability of acetylcholine receptors. *Dev. Biol.* 57:317–329.
7. Burden, S. 1977. Acetylcholine receptors at the neuromuscular junction: developmental change in receptor turnover. *Dev. Biol.* 61:79–85.
8. Bursztajn, S., and G. D. Fischbach. 1980. Accumulation of coated vesicles bearing α-BTX binding sites in brain treated myotubes. *Soc. Neurosci.* 6:358. (Abstr.)
9. Chang, C. C., and M. C. Huang. 1975. Turnover of junctional and extrajunctional acetylcholine receptors in the rat diaphragm. *Nature (Lond.).* 253:653–644.
10. Dennis, M. J. 1981. Development of the neuromuscular junction: inductive interactions between cells. *Annu. Rev. Neurosci.* 4:43–68.
11. Devreotes, P. N., and D. Fambrough. 1975. Acetylcholine receptor turnover in membranes of developing muscle fibers. *J. Cell Biol.* 65:335–358.
12. Drachman, D. B., C. W. Angus, R. N. Adams, and I. Kao. 1978. Effect of myasthenic patients' immunoglobulin on acetylcholine receptor turnover: selectivity of degradation process. *Proc. Natl. Acad. Sci. USA.* 75:3422–3426.
13. Ellisman, M. H., J. E. Rash, L. A. Staehelin, and K. R. Porter. 1976. Studies of excitable membranes. II. A comparison of specializations at neuromuscular junctions and non-junctional sarcolemmas of mammalian fast and slow twitch muscle fibers. *J. Cell Biol.* 68:752–774.
14. Fambrough, D. M. 1979. Control of acetylcholine receptors in skeletal muscle. *Physiol. Rev.* 59:165–227.
15. Fertuck, H. C., and M. M. Salpeter. 1974. Localization of acetylcholine receptor by ^{125}I-labeled α-bungarotoxin binding at mouse motor endplates. *Proc. Natl. Acad. Sci. USA.* 71:1376–1378.
16. Fertuck, H. C., and M. M. Salpeter. 1976. Quantitation of junctional and extrajunctional acetylcholine receptors by electron microscope autoradiography after ^{125}I-α-bungarotoxin binding at mouse neueromuscular junctions. *J. Cell Biol.* 69:144–158.
17. Fertuck, H. C., W. W. Woodward, and M. M. Salpeter. 1975. In vivo recovery of muscle contraction after α-bungarotoxin binding. *J. Cell Biol.* 66:209–213.
18. Heinemann, S., J. Merlie, and J. Lindstrom. 1978. Modulation of acetylcholine receptor at rat diaphragm by anti-receptor sera. *Nature (Lond.)* 274:65–68.
19. Land, B. R., E. E. Salpeter, and M. M. Salpeter. 1981. Kinetic parameters for acetylcholine interaction in intact neuromuscular junction. *Proc. Natl. Acad. Sci. USA.* 78:7200–7204.
20. Levitt, T. A., and M. M. Salpeter. 1981. Denervated endplates have a dual population of junctional acetylcholine receptors. *Nature (Lond.)* 291:239–241.
21. Loring, R. H., S. W. Jones, J. A. Matthews-Bellinger, and M. M. Salpeter. 1982. ^{125}I-α-bungarotoxin: the effect of radiodecomposition on specific activity. *J. Biol. Chem.* 257:1418–1423.
22. Loring, R. H., and M. M. Salpeter. 1980. Denervation increases turnover rate of junctional acetylcholine receptors. *Proc. Natl. Acad. Sci. USA.* 77:2293–2297.
23. Matthews-Bellinger, J., and M. M. Salpeter. 1978. Distribution of acetylcholine receptors at frog neuromuscular junctions with a discussion of some physiological implications. *J. Physiol. (Lond.)* 279:197–213.
24. Merlie, J. P., J. P. Changeux, and F. Gros. 1976. Acetylcholine receptor degradation measured by pulse chase labelling. *Nature (Lond.)* 264:74–76.
25. Michler, A., and B. Sakmann. 1980. Receptor stability and channel conversion in the subsynaptic membrane of the developing mammalian neuromuscular junction. *Dev. Biol.* 80:1–7.
26. Peper, K., F. Dreyer, C. Sandri, K. Akert, and H. Moor. 1974. Structure and ultrastructure of the frog motor endplate. A freeze etching study. *Cell Tissue Res.* 149:437–455.
27. Porter, C. W., and E. A. Barnard. 1975. The density of cholinergic receptors at the endplate postsynaptic membrane: ultrastructural studies in two mammalian species. *J. Membr. Biol.* 20:31–49.
28. Rash, J. E., and M. H. Ellisman. 1974. Studies of excitable membranes. I. Macromolecular specializations of the neuromuscular junction and the nonjunctional sarcolemma. *J. Cell Biol.* 63:567–586.
29. Rees, R. P. 1978. Inclusion in coated vesicle membrane as the transport mechanism for acetylcholine receptor molecules in isolated cultured sympathetic neurons. *J. Cell Biol.* 79(2, Pt. 2):99*a*. (Abstr.)
30. Reiness, C. G., and C. B. Weinberg. 1981. Metabolic stabilization of acetylcholine receptors at newly formed neuromuscular junctions in rat. *Dev. Biol.* 84:247–254.
31. Reiness, C. G., C. B. Weinberg, and Z. H. Hall. 1978. Antibody to acetylcholine receptor increases degradation of junctional and extrajunctional receptors in adult muscles. *Nature (Lond.).* 274:68–70.
32. Salpeter, M. M. 1981. High Resolution Autoradiography. *In* Techniques in the Life Sciences. Techniques in Cellular Physiology. Part I. Elsevier North-Holland Scientific Publishers Ltd., County Clare, Ireland. Vol. P1/I (P106):1–45.
33. Salpeter, M. M., and L. Bachmann. 1964. Autoradiography with the electron microscope, a procedure for improving resolution, sensitivity, and contrast. *J. Cell Biol.* 22:469–477.
34. Salpeter, M. M., and L. Bachmann. 1972. Electron microscope autoradiography. *In* Principles and Techniques of Electron Microscopy, Biological Applications. M. A. Hayat, editor. Van Nostrand Reinhold Co., New York. 2:221–278.
35. Salpeter, M. M., and M. G. Farquhar. 1981. High resolution analysis of the secretory pathway in mammatrophs of the rat anterior pituitary. *J. Cell Biol.* 91:240–246.
36. Salpeter, M. M., F. A. McHenry, and E. E. Salpeter. 1978. Resolution in electron microscope autoradiography. IV. Application to analysis of autoradiograms. *J. Cell Biol.* 76:127–145.
37. Salpeter, M. M., S. Spanton, K. Holley, and T. R. Podleski. 1982. Brain extract causes acetylcholine receptor redistribution which mimics some early events at developing neuromuscular junctions. *J. Cell Biol.* 93:417–425.
38. Shainberg, A., and M. Burstein. 1976. Decrease of acetylcholine receptor synthesis in muscle cultures by electrical stimulation. *Nature (Lond.).* 264:368–369.
39. Stanley, E. F., and D. B. Drachman. 1978. Effect of myasthenic immunoglobulin on acetylcholine receptors of intact mammalian neuromuscular junctions. *Science (Wash. DC).* 200:1285–1287.
40. Stanley, E. F., and D. B. Drachman. 1982. Newly inserted ACh receptors at the neuromuscular junction have a fast rate of degradation. *Soc. Neurosci.* 8(Pt. I):185. (Abstr.)
41. Steinbach, J. H., J. H. Merlie, S. Heinemann, and R. Block. 1979. Degradation of junctional and extrajunctional acetylcholine receptors by developing rat skeletal muscle. *Proc. Natl. Acad. Sci. USA.* 76:3547–3551.
42. Weinberg, C. B., C. G. Reiness, and Z. W. Hall. 1981. Topographical segregation of old and new acetylcholine receptors at developing ectopic endplates in adult rat muscle. *J. Cell Biol.* 88:215–218.